Structural Stability against Disintegration by Anionic Lipids Rationalizes the Efficiency of Cationic Liposome/DNA Complexes

Giulio Caracciolo,*,† Cristina Marchini,‡ Daniela Pozzi,† Ruggero Caminiti,†
Heinz Amenitsch,§ Maura Montani,‡ and Augusto Amici‡

*Department of Chemistry, University of Rome "La Sapienza", P.le A. Moro 5, 00185 Rome, Italy, Genetic
Immunization Laboratory, Department of Molecular Cellular and Animal Biology, University of Camerino,
Via Camerini 5, 62032 Camerino (MC), Italy, and Institute of Biophysics and Nanosystems Research,
Austrian Academy of Sciences, Schmiedelstrasse 6, A-8042 Graz, Austria*

Reported here is the correlation between the transfection efficiency of cationic liposome/DNA complexes (lipoplexes) and the structural evolution that they undergo when interacting with anionic membrane lipids. Multicomponent lipoplexes, incorporating from three to six lipid species simultaneously, presented a much higher transfection efficiency than binary lipoplexes, which are more commonly used for gene-delivery purposes. The discovery that a high transfection efficiency can be achieved by employing multicomponent complexes at a lower-than-ever-before membrane charge density of lipoplexes was of primary significance. Synchrotron small-angle X-ray diffraction (SAXD) experiments showed that anionic liposomes made of dioleoylphosphatidylglycerol (DOPG) disintegrated the lamellar phase of lipoplexes. DNA unbinding was measured by electrophoresis on agarose gels. Most importantly, structural changes induced by anionic lipids strictly depended on the lipid composition of lipoplexes. We found evidence of the existence of three different regimes of stability related to the interaction between complexes and anionic membranes. Both unstable (with low membrane charge density, σ_M) and highly stable lipoplexes (with high σ_M) exhibited low transfection efficiency whereas highly efficient multicomponent lipoplexes exhibited an "optimal stability". This intermediate regime reflects a compromise between two opposing constraints: protection of DNA in the cytosol and endosomal escape. Here we advance the concept that structural stability, upon interaction with cellular anionic lipids, is a key factor governing the transfection efficiency of lipoplexes. Possible molecular mechanisms underlying experimental observations are also discussed.

Introduction

Non-viral gene-delivery strategies have received much attention since ground-breaking studies by Felgner et al.[1] showed how complexes composed of cationic liposomes (CLs, self-closed lipid vesicles made of cationic and neutral lipids) and DNA, named lipoplexes, could serve as gene-delivery vehicles in the targeting of extracellular DNA into cell nuclei. Widespread application for lipoplexes has been found in molecular cell biology, with the main advantages with respect to viral vectors being low toxicity, easy of production, and high DNA packing density. The possibility of carrying DNA of a much larger size and of targeting lipid carriers to specific cell types makes them more attractive candidates for gene delivery than their viral counterparts.[2]

Formulations based on the exclusive use of zwitterionic lipids have also been investigated.[3,4] In that case, divalent electrolyte counterions common in biological cells ($Mn^{2+}, Ca^{2+}, Co^{2+}, Mg^{2+}, Fe^{2+}$) serve as DNA condensing agents.[3,4] In these complexes, a high level of DNA organization (i.e., a rectangular columnar phase) was observed.[5] This finding was extremely significant in view of recent interest in creating new synthetic systems at the interface of biology. Within this framework, some of us reported on a new experimental procedure resulting in the formation of solid-supported DNA−Mn^{2+}−lipid complexes under the biologically relevant excess water condition.[6] These innovative biomaterials do not exhibit cytotoxicity but, unfortunately, are currently less stable and less efficient than cationic liposome−DNA complexes.

As with most synthetic transfection systems, the use of lipoplexes is limited by our insufficient understanding of the formation mechanism, the structure, and the stability of the complexes and, most importantly, the manner in which they cross cell membranes and how they are relieved of their genetic freight.[7] Knowledge of the correlation between the physical attributes of these complexes and their functional activity is crucial to improving them as efficient synthetic carriers of genes. A critical requirement for enhancing transfection efficiency (TE) is, for example, a full understanding of the different nanostructures of lipoplexes.[2] Over the last few years, it has been shown[8−12] that lipoplexes form an ordered liquid-crystalline multilamellar structure (L_α^C phase) with DNA condensed between opposing

* Corresponding author. E-mail: g.caracciolo@caspur.it. Tel: + 39 06 4991 3076. Fax: +39 06 490631.
† University of Rome.
‡ University of Camerino.
§ Austrian Academy of Sciences.

(1) Felgner, P. L.; Ringold, G. M. *Nature* **1989,** *331,* 461.
(2) Safinya, C. R. *Curr. Opin. Struct. Biol.* **2001,** *11,* 440.
(3) McManus, J. J.; Rädler, J. O.; Dawson, K. A. *Langmuir* **2003,** *19,* 9630.
(4) McManus, J. J.; Rädler, J. O.; Dawson, K. A. *J. Phys. Chem. B* **2003,** *107,* 9869.
(5) McManus, J. J.; Rädler, J. O.; Dawson, K. A. *J. Am. Chem. Soc.* **2004,** *126,* 15966.

(6) Caracciolo, G.;. Sadun, C.; Caminiti, R.; Pisani, M.; Bruni, P.; Francescangeli, O. *Chem. Phys. Lett.* **2004,** *397,* 138.
(7) Ewert, K. K.; Ahmad, A.; Evans, H. M.; Safinya, C. R. *Expert Opin. Biol. Ther.* **2005,** *5,* 33.
(8) Salditt, T.; Koltover, I.; Rädler, J. O.; Safinya, C. R. *Phys. Rev. Lett.* **1997,** *79,* 2582.
(9) Salditt, T.; Koltover, I.; Rädler, J. O.; Safinya, C. R. *Phys. Rev. E* **1998,** *58,* 889.
(10) Koltover, I.; Salditt, T.; Rädler, J. O.; Safinya, C. R. *Science* **1998,** *281,* 78.
(11) Artzner, F.; Zantl, R.; Rapp, G.; Rädler, J. O. *Phys. Rev. Lett.* **1998,** *81,* 5015.
(12) Caracciolo, G.; Caminiti, R.; Pozzi, D.; Friello, M.; Boffi, F.; Congiu, Castellano, A. *Chem. Phys. Lett.* **2002,** *351,* 222.
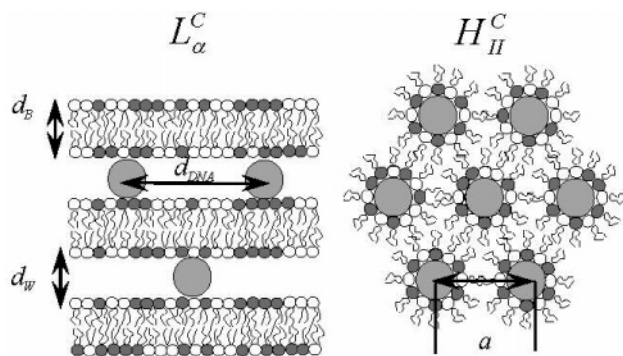
Figure 1. Schematics of the inner structure of lamellar and hexagonal CL−DNA complexes. The lamellar phase, L_α^C, is composed of alternative lipid bilayers and DNA monolayers, with the repeat spacing given by $d = d_W + d_B$. The hexagonal phase, H_{II}^C, is composed of cylinders consisting of DNA coated with a lipid monolayer arranged on a hexagonal lattice.

cationic lipid membranes or, alternatively, an inverted hexagonal H_{II}^C phase composed of lipid-coated DNA strands arranged on a hexagonal lattice (Figure 1). A third phase of lipoplexes was recently described by Ewert et al.[13] This novel lattice structure, termed H_I^C, is composed of hexagonal lipid micelles surrounded by DNA strands forming a 3D substrcuture. It was first hypothesized[10] that a direct connection between the lipoplex structure and TE existed, leading to the misconception that H_{II}^C lipoplexes transfected more efficiently than L_α^C ones. When experimental evidence was provided that lamellar complexes could compete in TE with hexagonal ones,[14,15] it became clear that many other aspects of lipoplex-mediated transfection needed to be investigated.[14,16] Among physical chemical parameters affecting TE, the membrane charge density (i.e., the average charge per unit area of the lipid membrane, σ_M) has recently been identified as a universal parameter that governs the TE behavior of lamellar complexes in vitro.[17] In particular, the existence of an optimal membrane charge density, σ_M^*, was demonstrated, and TE data were found to merge onto a universal, bell-shaped curve as a function of σ_M.[17] More recently, the unbinding of DNA from a lipoplex after entering the cell has been identified as one of the key steps in lipid-mediated DNA delivery (lipofection).[18] A number of investigators observed the release of DNA molecules from various lipoplexes after treatment with anionic lipids (ALs).[19−21] Experiments have clarified that the unbinding is a result of charge neutralization by cellular anionic lipids[20,22] and have also suggested that structural changes in lipoplexes may be a controlling factor in DNA delivery.[18]

To test this idea, we investigated the correlation between TE and the structural evolution of lipoplexes upon interaction with cellular (anionic) lipids. To this end, we used both binary and multicomponent (MC) lipoplexes.[23,24] In contrast to binary lipoplexes, MC lipoplexes incorporate more than two lipid species within the lipid bilayer, with different headgroups and a number of systematic variations in relevant physical−chemical parameters.[23,24] We applied small-angle synchrotron X-ray diffraction (SAXD) to study the structural correlations of the lipoplex formulations and their mixtures with anionic lipids. Electrophoresis experiments were carried out to measure the extent of DNA unbinding. In actuality, the DNA-releasing capacity of different formulations of lipoplexes varied considerably. On the basis of our combined TE and structural results, we put forth the concept that the structural stability of lipoplexes against anionic lipids is the determining factor in lipofection.

Materials and Methods

Liposome Preparation. Cationic 1,2-dioleoyl-3-trimethylammonium-propane (DOTAP) and 3β-[N-(N′,N′-dimethylaminoethane)-carbamoyl]-cholesterol (DC-Chol), anionic dioleoylphosphatidylglycerol (DOPG) and neutral dioleoylphosphatidylethanolamine (DOPE), dioleoylphosphocholine (DOPC), 1,2-dilauroyl-*sn*-glycero-3-phosphocholine (DLPC), and 1,2-dimyristoyl-*sn*-glycero-3-phosphocholine (DMPC) were purchased from Avanti Polar Lipids (Alabaster, AL) and used without further purification. DOTAP−DOPC (A), DC-Chol−DOPE (B), DOTAP−DLPC (C), DC-Chol−DMPC (D), and DOTAP−DOPE (E) CLs were routinely prepared.[12] In brief, each binary mixture, at a molar ratio of neutral lipid in the bilayer Φ = (neutral lipid/total lipid) (mol/mol) = 0.5, was dissolved in chloroform, and the solvent was evaporated in vacuum for at least 24 h. The obtained lipid films were hydrated with the appropriate amount of Tris-HCl buffer solution (10^{-2} M, pH 7.4) to achieve the desired final concentration (∼25 mg/mL for X-ray samples). The solutions were incubated at 30 °C for 6 h to allow for the formation of CLs. The obtained liposome solutions were then stored at 30 °C for 24 h to achieve full hydration. Indeed, we have recently found evidence that lipid hydration is the key factor regulating the equilibrium structure of lipoplexes.[25] The same protocol was followed to prepare anionic DOPG liposomes. To facilitate the X-ray diffraction measurements, DOPG liposomes were transferred to 1.5-mm-diameter quartz X-ray capillaries (Hilgenberg, Germany). The capillaries were centrifuged at room temperature for 5 min at a speed of 6000 rpm to consolidate the sample.

Lipoplex Preparation. Calf thymus Na-DNA was purchased from Sigma (St. Louis, MO). DNA was dissolved in Tris-HCl buffer and was sonicated for 5 min, inducing DNA fragmentation with a length distribution between 500 and 1000 base pairs, which was determined by gel electrophoresis. Lipoplexes were prepared by mixing 100 μL of calf thymus DNA at 5.3 mg/mL with suitable volumes of A, B, C, D, and E liposome solutions. As a result, DOTAP−DOPC/DNA (A/DNA), DC-Chol−DOPE/DNA (B/DNA), DOTAP−DLPC/DNA (C/DNA), DC-Chol−DMPC/DNA (D/DNA), and DOTAP−DOPE/DNA (E/DNA) binary lipoplexes were obtained. Multicomponent lipoplexes were prepared by adding DNA to mixed lipid dispersions made of distinct populations of CLs. As a result, multicomponent lipoplexes formed in a self-assembled manner.[23,24] Samples were prepared in the following cationic lipid/DNA ratios (ρ = cationic lipid (by mole)/DNA base): 0 (pure lipid) and 3.2 (positively charged lipoplexes). After storage for 3 days at 4 °C, allowing the samples to reach equilibrium, they were transferred to 1.5-mm-diameter quartz X-ray capillaries (Hilgenberg, Germany). The capillaries were centrifuged at room temperature for 5 min at

(13) Ewert, K. K.; Evans, H. M.; Zidovska, A.; Bouxsein, N. F.; Ahmad, A.; Safinya, C. R. *J. Am. Chem. Soc.* **2006**, *128*, 3998.

(14) Caracciolo, G.; Pozzi, D.; Caminiti, R.; Congiu, Castellano, A. *Eur. Phys. J. E* **2003**, *10*, 331.

(15) Lin, A. J.; Slack, N. L.; Ahmad, A.; George, C. X.; Samuel, C. E.; Safinya, C. R. *Biophys. J.* **2003**, *84*, 3307.

(16) Koynova, R.; Wang, L.; MacDonald, R. C. *Proc. Natl. Acad. Sci. U.S.A.* **2006**, *103*, 14373.

(17) Ahmad, A.; Evans, H. M.; Ewert, K.; George, C. X.; Samuel, C. E.; Safinya, C. R. *J. Gene Med.* **2005**, *7*, 739.

(18) Koynova, R.; Wang, L.; Tarahovsky, Y.; MacDonald, R. C. *Bioconjugate Chem.* **2005**, *16*, 1335.

(19) MacDonald, R. C.; Ashley, G. W.; Shida, M. M.; Rakhmanova, V. A.; Tarahovsky, Y. S.; Pantazatos, D. P.; Kennedy, M. T.; Pozharski, E. V.; Baker, K. A.; Jones, R. D.; Rosenzweig, H. S.; Choi, K. L.; Qiu, R. Z.; McIntosh, T. J. *Biophys. J.* **1999**, *77*, 2612.

(20) Xu, Y. H.; Szoka, F. C. *Biochemistry* **1996**, *35*, 5616.

(21) Tarahovsky, Y.; Koynova, R.; MacDonald, R. C. *Biophys. J.* **2004**, *86*, 37A.

(22) Caracciolo, G.; Pozzi, D.; Caminiti, R.; Marchini, C.; Montani, M; Amici, A; Amenitsch, H. *Appl. Phys. Lett.* **2006**, *89*, 233903.

(23) Caracciolo, G.; Pozzi, D.; Amenitsch, H.; Caminiti, R. *Langmuir* **2005**, *21*, 11582.

(24) Caracciolo, G.; Pozzi, D.; Caminiti, R.; Amenitsch, H. *Appl. Phys. Lett.* **2005**, *87*, 133901.

(25) Pozzi, D.; Amenitsch, H.; Caminiti, R.; Caracciolo, G. *Chem. Phys. Lett.* **2006**, *429*, 250.

Table 1. Lipid Composition, Membrane Charge Density, σ_M, and Transfection Efficiency (TE) of Lipoplexes Used[a]

lipid composition	X_{DOTAP}	$X_{DC-Chol}$	X_{DOPC}	X_{DOPE}	X_{DMPC}	X_{DLPC}	$\sigma_M\ 10^{-3}$ (e/Å²)	TE (RLU/mg)	ΔTE (RLU/mg)
A	0.5	0	0.5	0	0	0	7.6	1.8×10^7	8×10^6
AC	0.5	0	0.25	0	0	0.25	7.6	1.5×10^7	9×10^6
C	0.5	0	0	0	0	0.5	7.9	1.3×10^7	5×10^6
AE (1:4)	0.1	0.4	0.5	0	0	0	8.1	1.0×10^8	2×10^7
AE (2:3)	0.5	0	0.2	0.3	0	0	8.2	4.9×10^8	4×10^7
CD	0.25	0.25	0	0	0.25	0.25	8.4	1.9×10^8	1×10^7
ABCD	0.25	0.25	0.125	0.125	0.125	0.125	8.5	7.8×10^8	9×10^7
AB	0.25	0.25	0.25	0.25	0	0	8.5	8.1×10^8	1×10^8
ABCD (1:2:1:1)	0.2	0.3	0.1	0.2	0.1	0.1	8.7	5.6×10^8	1×10^8
ABCD (1:3:1:1)	0.17	0.33	0.08	0.25	0.08	0.08	8.9	1.2×10^9	2×10^8
EB (1:4)	0.1	0.4	0	0.5	0	0	9.4	6.2×10^8	5×10^7
D	0	0.5	0	0	0.5	0	9.4	1.9×10^7	3×10^6
BD	0	0.5	0	0.25	0.25	0	9.6	1.6×10^8	2×10^7
B	0	0.5	0	0.5	0	0	9.8	6.4×10^7	3×10^7

[a] X_i is the molar fraction of the *i*th lipid species of which the lipid bilayer is composed ($\sum_{i=1}^{6} X_i = 1$). Samples are listed as a function of increasing σ_M. Where not specified, liposomes were in an equimolar ratio.

6000 rpm to consolidate the sample. All lipoplexes prepared are listed in Table 1.

Lipoplex/Anionic Liposome Systems. Lipoplexes and anionic liposomes were mixed at seven anionic/cationic charge ratios ($R = 0, 0.1, 0.2, 0.5, 1, 5, 10, 20$). These mixed dispersions were then equilibrated for 2 days, placed in quartz capillaries, and flame-sealed. SAXD measurements allowed us to estimate the R range where lipoplex disintegration occurred. Such ranges are strictly dependent on the specific lipoplex formulation employed. Further finer measurements carried out in such ranges allowed us to determine accurately the anionic/cationic charge ratio, R^*, at which the disintegration of lamellar lipoplex was complete.

Transfection Efficiency Experiments. Cell lines were cultured in Dulbecco's modified Eagle's medium (DMEM, Invitrogen) supplemented with 1% penicillin−streptomycin (Invitrogen) and 10% fetal bovine serum (FBS, Invitrogen) at 37 °C in a 5% CO$_2$ atmosphere, splitting the cells every 2−4 days to maintain monolayer coverage. For luminescence analysis, NIH 3T3 and A17 cells were transfected with pGL3 control plasmid (Promega), which codes for firefly luciferase. The day before transfection, cells were seeded in 24 well plates (150.000 cells/well) using an antibiotic-free medium. Cells were incubated until they were 75−80% confluent, which generally took 18 to 24 h. On the day of transfection, the medium containing serum was removed from the well plates and replaced with a transfection medium without serum (Optimem I, Invitrogen). For TE experiments, lipoplexes were prepared by adding 0.5 μg of plasmid in 50 μL of Optimem with 5 μL of lipid dispersions (1 mg/mL) in 50 μL of Optimum. These complexes were left at room temperature for 20 min before adding them to the cells. The cells were incubated with lipoplexes in Optimem (Invitrogen) for 6 h to permit transient transfection; the medium was then replaced with DMEM supplemented with FBS. Luciferase expression was analyzed after 48 h and measured with the luciferase assay system from Promega, and light output measurements were performed on a Berthold LB-953 AutoLumat luminometer (Berthold). TE was normalized to milligrams of total cellular protein in the lysates using the Bio-Rad protein assay dye reagent (Bio-Rad).

Synchrotron Small-Angle X-ray Diffraction Measurements. All SAXD measurements were performed at the Austrian SAXS station of the synchrotron light source ELETTRA (Trieste, Italy).[26] SAXD patterns were recorded with a gas detector based on the delay line principle covering a q range of between 0.05 and 1.5 Å^{-1}. The angular calibration of the detector was performed with silver behenate [CH$_3$(CH$_2$)$_{20}$-COOAg] whose d value corresponds to 58.38 Å. Exposure times for every sample were 300 s. No evidence of sample degradation due to radiation damage was observed in any of the samples at this exposure. The data have been normalized for primary beam intensity and detector efficiency, as well as having the

background subtracted. Temperature was controlled in the vicinity of the capillary to within ±0.1 °C (Anton Paar, Graz, Austria).

Data Analysis. From the synchrotron SAXD patterns we could calculate electron density profiles (EDPs) along the normal to lipid bilayers. The electron density profile, $\Delta\rho$, can be calculated as a Fourier sum of cosine terms,[27−28]

$$\Delta\rho = \frac{\rho(z) - \langle\rho\rangle}{[\langle\rho^2(z)\rangle - \langle\rho\rangle^2]^{1/2}} = \sum_{l=1}^{N} F_l \cos\left(2\pi l \frac{z}{d}\right) \quad (1)$$

where $\rho(z)$ is the electron density, $\langle\rho\rangle$ is its average value, N is the highest order of the Bragg reflection observed in the SAXD pattern, F_l is the form factor for the (00*l*) reflection, and d is the lamellar repeat spacing along the normal to the lipid bilayer. The phase choice for each lipid mixture (i.e., the correct sign combination used to calculate the electron density profile) was found so that the profiles exhibited the usual lipid bilayer density plus an additional maximum in the middle of the water region due to the DNA chains.[25,28−31]

DNA Release Measured by Electrophoresis. Electrophoresis studies were conducted on 1% agarose gels containing ethidium bromide in Tris-borate-EDTA (TBE) buffer. Lipoplexes were prepared by mixing 40 μL of lipid dispersions (∼1 mg/mL, Tris-HCl buffer) with 4 μg of pGL3 control plasmid. These complexes were allowed to equilibrate for 3 days at 4 °C before adding negatively charged liposomes. After 48 h, naked plasmid DNA, lipoplexes, and lipoplexes/AL systems with different R values were analyzed by electrophoresis. For this purpose, 20 μL of each sample was mixed with 4 μL of loading buffer (glycerol 30%, bromophenol blue 0.25%) and subjected to agarose gel electrophoresis for 1 h at 80 V. The electrophoresis gel was visualized and digitally photographed using a Kodak Image Station, model 2000 R (Kodak, Rochester, NY). Digital photographs were enhanced using dedicated software (Kodak MI, Kodak).

Results and Discussion

Synchrotron SAXD experiments clarified the structure of lipoplexes. All lipoplexes formed the lamellar L_α^C phase (Figure 1). Figure 2 shows typical SAXD patterns of binary (A/DNA, B/DNA, C/DNA and D/DNA) and multicomponent (AB/DNA

(26) Amenitsch, H.; Rappolt, M.; Kriechbaum, M.; Mio, H.; Laggner, P.; Bernstorff, S. *J. Synchrotron Radiat.* **1998**, *5*, 506.

(27) Luzzati, V.; Mariani, P.; Delacroix, H. *Makromol. Chem., Macromol. Symp.* **1998**, *15*, 1.

(28) Francescangeli, O.; Rinaldi, D.; Laus, M.; Galli, G.; Gallot, B. *J. Phys. II France* **1996**, *6*, 77.

(29) Zantl, R.; Artzner, F.; Rapp, G.; Rädler, J. O. *Europhys. Lett.* **1998**, *45*, 90.

(30) Zantl, R.; Baicu, L.; Artzner, F.; Sprenger, I.; Rapp, G.; Rädler, J. O. *J. Phys. Chem. B* **1999**, *103*, 10300.

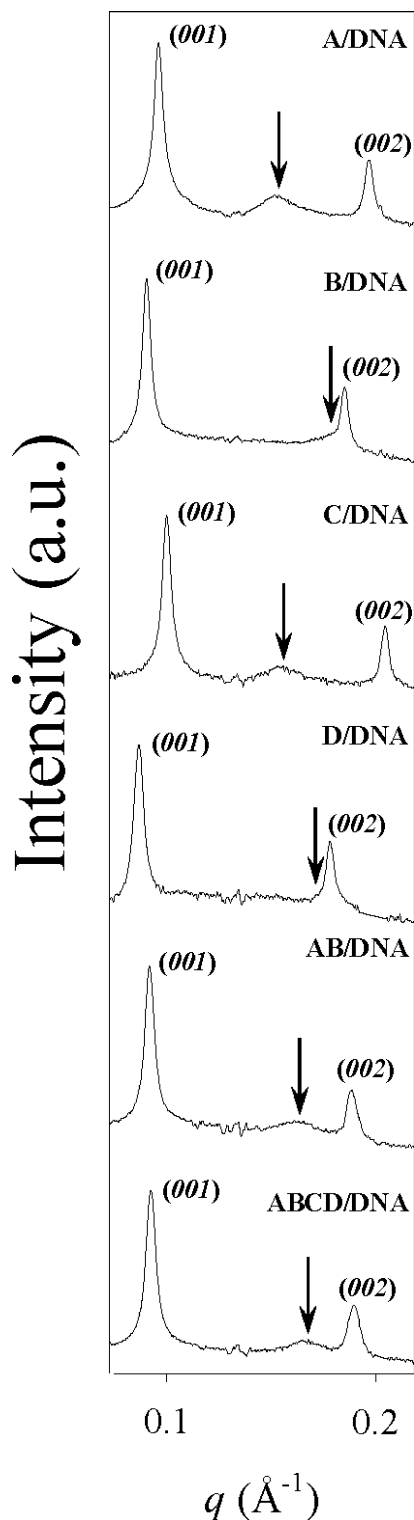(31) Caracciolo, G.; Pozzi, D.; Amenitsch, H.; Caminiti, R. *Langmuir* **2006**, *22*, 4267.

Figure 2. Representative SAXD patterns of lipoplexes as a function of increasing number of lipid components: DOTAP−DOPC/DNA (A/DNA), DC-Chol−DOPE/DNA (B/DNA), DOTAP−DLPC/DNA (C/DNA), DC-Chol−DMPC/DNA (D/DNA), DOTAP−DC-Chol−DOPC−DOPE/DNA (AB/DNA), and DOTAP−DC-Chol−DOPC−DOPE−DLPC−DMPC/DNA (ABCD/DNA). The DNA−DNA mobile peak is marked by an arrow and shifts as a function of lipid composition as a result of the change in the membrane charge density.

lamellar periodicity along the normal to the lipid bilayer, d, which is the sum of the membrane thickness (d_B) and the thickness of the water/DNA layer (d_W): $d = d_B + d_W = 2\pi/q_{001}$ (Figure 1). The diffuse broader peak (marked by an arrow) resulted from 1D ordering of the DNA sandwiched between the lipid bilayers and corresponded to a DNA interhelical spacing of $d_{DNA} = 2\pi/q_{DNA}$ (Figure 1). It is worth mentioning that we observed that each SAXD pattern arose from a single lamellar phase with a distinct DNA packing density (i.e., a single DNA peak appeared on the diffraction pattern). This means that the structure of multicomponent lipoplexes was likely to be unique with lipid species ideally mixed within the membrane. Figure 2 also shows that the DNA peak was mobile as a function of lipid composition (i.e., as a function of the number and kind of lipid molecules of which the lipid bilayers were composed). Because the membrane charge density of lipid membranes, σ_M, is the only physical constraint regulating DNA packing density within lipid/DNA complexes,[32−35] this means that adjusting the lipid composition of multicomponent lipoplexes may induce the formation of cationic membranes with specific surface charge densities.

Remembering that multicomponent lipoplexes were prepared by adding DNA to mixed dispersions made of two or three coexisting populations of binary CLs, our SAXD findings imply that binary CLs broke up during lipoplex formation and that complete lipid mixing at the molecular level occurred. We emphasize that several energy barriers opposing the mixing process exist.[36] Indeed, positive electrostatic charges localized on the surface of CLs create a repulsive barrier that dominates over short-range attractive van der Waals forces and prevents membrane aggregation and fusion. Furthermore, lipid molecules are held in bilayer vesicles by hydrophobic interactions, and a change in supramolecular organization, which is required by the mixing process, is opposed by this strong energy barrier. SAXD experiments showed that (data not reported) in the absence of DNA no fusion between coexisting cationic lipid vesicles occurred. Conversely, when DNA was added, the mixing process took place spontaneously and multicomponent lipoplexes formed in a self-assembled manner. This indicates that DNA acted as a fusogenic agent favoring the apposition of lipid vesicles and contact and fusion[37−39] by reducing the energy barrier due to electrostatic, hydrophobic, steric, and hydration interactions. Then, the fluid lipid bilayer allowed for the lateral diffusion of lipid molecules, leading to a spatial distribution of the lipid species that on average is uniform. Hence, SAXD experiments allowed us to clarify the microscopic mechanisms driving the formation of multicomponent lipoplexes and to detect the ability of DNA to mix the lipids completely (Figure 3).

Figure 4 shows the EDP of A/DNA lipoplexes with a large central minimum corresponding to the region of the lipid hydrocarbon tails plus two strong maxima due to the lipid polar headgroups. The distance between the maxima of EDP gives a good estimate of the lipid bilayer thickness, d_B, whereas the water-layer thickness is defined as $d_W = d - d_B$. The EDP of Figure 4 shows the usual features of lipid bilayer density whereas

and ABCD/DNA) lipoplexes at a fixed cationic lipid/DNA charge ratio of $\rho = 3.2$ with no anionic lipid added. The charge ratio of $\rho = 3.2$ was chosen because it corresponds to the middle of a typical plateau region observed for optimal transfection conditions.[7,15] The sharp peaks labeled at q_{00l} arose from the

(32) Koltover, I.; Salditt, T.; Safinya, C. R. *Biophys. J.* **1999**, *77*, 915.
(33) Koltover, I.; Wagner, K.; Safinya, C. R. *Proc. Natl. Acad. Sci. U.S.A.* **2000**, *97*, 14046.
(34) Caracciolo, G.; Caminiti, R. *Chem. Phys. Lett.* **2004**, *400*, 314.
(35) Huebner, S.; Battersby, B. J.; Grimm, R.; Cevc, G. R. *Biophys. J.* **1999**, *76*, 3158.
(36) Caracciolo, G.; Pozzi, D.; Caminiti, R.; Amenitsch, H. *Chem. Phys. Lett.* **2006**, *429*, 250.
(37) Hayes, M. E.; Gorelov, A. V.; Dawson, K. A. *Prog. Colloid Polym. Sci.* **2001**, *118*, 243.
(38) Barreleiro, P. C. A.; May, R. P.; Lindman, B. *Faraday Discuss.* **2002**, *122*, 191.
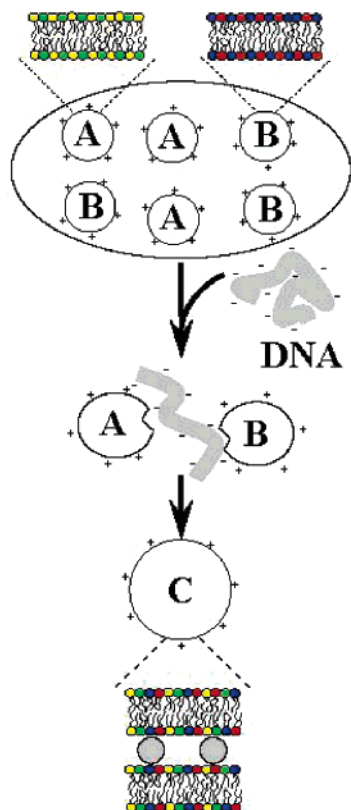(39) Barreleiro, P. C. A.; Lindman, B. *J. Phys. Chem. B* **2003**, *107*, 6208.

Figure 3. Mechanism of formation of mixed multicomponent lipoplexes. (For clarity, each color refers to a single lipid species.) In the first step, DNA is added to a mixed dispersion containing positively charged A and B binary cationic liposomes. Each kind of liposomes is a binary mixture of cationic and neutral lipids. In the second step, DNA induces the local aggregation and fusion of A and B liposomes. Upon DNA-induced fusion of liposomes, multicomponent lipoplexes (C) form with four lipid species ideally mixed.

Table 2. Lamellar d Spacing, Lipid Bilayer Thickness, d_B, Water Layer Thickness, d_W, and DNA$-$DNA Distance, d_{DNA}, of DOTAP$-$DOPC/DNA (A/DNA), DC-Chol$-$DOPE/DNA (B/DNA), and of Multicomponent Lipoplexes (AB/DNA), Incorporating the Four Lipid Species within the Lipid Bilayer[a]

	d (Å)	d_B (Å)	d_W (Å)	d_{DNA} (Å)
A/DNA	64.6	38.4	26.2	42.6
AB/DNA	66.1	39.8	26.3	41.4
B/DNA	67.9	41.6	26.3	38.1

[a] Structural parameters were calculated from the EDPs.

the 1D DNA in-plane rod lattice is responsible for the increase in electron density at the edges of the EDP. Structural parameters derived from the EDPs are reported in Table 2 for three selected samples, two binary lipoplexes, and the four-component lipoplex incorporating all four lipid species. Table 2 shows that physical properties of multicomponent lipoplexes were intermediate between those of binary lipoplexes and might therefore be adjusted merely by varying their lipid composition. This was a relevant result because it opened the gateway to prepare lipid/DNA complexes with rationally designed physical properties. In the future, rationally designed vectors shall incorporate the most useful elements of synthetic systems with variations depending on their specific application.[40]

With the aim of investigating the structure/activity relationship of lipoplexes, we performed a transient transfection assay of
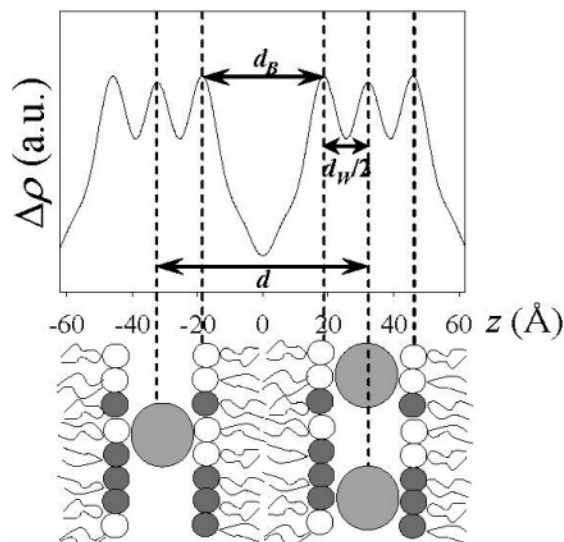
(40) Rubanyi, G. M. *Mol. Aspects Med.* **2001**, 22, 113.

Figure 4. Electron density profile of DOTAP$-$DOPC/DNA (A/DNA) lipoplexes. The high-electron-density region, corresponding to the main maxima, reflects the presence of the phospholipid headgroups, and the low-electron-density region reflects the hydrocarbon chains. Bilayer parameters are defined: d, lamellar repeat distance; d_B, bilayer region thickness; and d_W, interlamellar water layer thickness. Two secondary maxima at the edges of the profile are observed, corresponding to the embedded DNA molecules.

mouse fibroblast cell lines (NIH 3T3). Figure 5 shows the TE, reported as relative light units (RLU) per milligram of total protein content, plotted versus the membrane charge density, σ_M. Each TE data point in Figure 5 represents an average value of at least four experimental observations. Errors for TE are listed in Table 1. We calculated σ_M according to Lin et al.,[15] with σ_M = total charge/total membrane area. In our case, the matter was complicated by the presence of more than two lipid species within the lipid bilayer. As a consequence, the membrane charge density reads

$$\sigma_M = \frac{\sum_{i=1}^{N} Z_i e n_i^+}{\sum_{i=1}^{N} n_i^+ A_i^+ + \sum_{j=1}^{M} n_j^0 A_j^0} \quad (2)$$

where n_i^+ is the number of cationic lipids of the ith species with valence Z_i and head group area A_i^+, n_j^0 is the number of neutral lipids of the jth species with head group area A_j^0, and N and M are the number of cationic and neutral lipid species in the lipid bilayer, respectively. For our data, we used $A_{DOTAP} = 68$ Å²,[41] $A_{DC-Chol} = 41.4$ Å²,[42] $A_{DOPC} = 72$ Å²,[43] $A_{DOPE} = 55.1$ Å²,[44] $A_{DMPC} = 60.6$ Å²,[45] and $A_{DLPC} = 63.2$ Å².[45] In Table 1 under lipid composition, membrane charge density as calculated by eq 2 and the TE values of all of the lipoplexes used are listed. Figure 6 shows the DNA interdistance against σ_M as calculated by eq 2. Uncertainties for σ_M were calculated from eq 2 using standard error propagation, with errors for the lipid headgroup areas being obtained from ref 41−45. As expected,[25,31,33] the 1D DNA packing

(41) Caminiti, R.; Caracciolo, G.; Pisani, M.; Bruni, P. *Chem. Phys. Lett.* **2005**, 409, 331.
(42) Radhakrishnan, A.; Li, X. M.; Brown, R. E.; McConnell, H. M. *Biochim. Biophys. Acta* **2001**, 1551, 1.
(43) Tristram-Nagle, S.; Petrache, H. I.; Nagle, J. F. *Biophys. J.* **1998**, 75, 917.
(44) Huang, P.; Perez, J. J.; Loew, G. H. *J. Biomol. Struct. Dyn.* **1994**, 11, 927.
(45) Kucerka, N.; Liu, Y.; Chu, N.; Petrache, H. I.; Tristram-Nagle, S.; Nagle, J. F. *Biophys. J.* **2005**, 88, 2626.
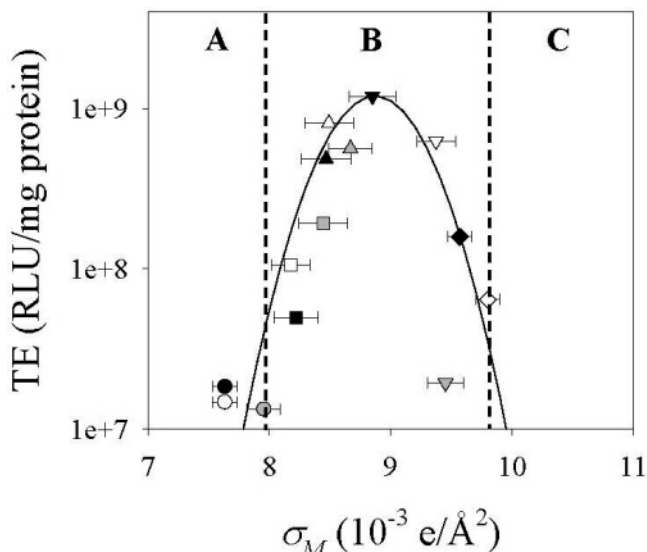
Figure 5. TE in RLU per milligram of cellular protein plotted as a function of the membrane charge density of lipid membranes, σ_M. Each symbol refers to a specific lipoplex: DOTAP−DOPC/DNA (black circle), DOTAP−DOPC−DLPC/DNA (white circle), DOTAP−DLPC/DNA (gray circle), DOTAP−DOPC−DOPE/DNA (black square, lipid species in a 5:1:4 molar ratio), DOTAP−DOPC−DOPE/DNA (white square, lipid species in a 5:2:3 molar ratio), DOTAP−DLPC−DMPC (gray square), DOTAP−DOPC−DLPC−DC-Chol−DOPE−DMPC (black up-triangle, lipid species in a 2:1:1:2:1:1 molar ratio), DOTAP−DOPC−DC-Chol−DOPE (white up-triangle), DOTAP−DOPC−DLPC−DC-Chol−DOPE−DMPC (gray up triangle, lipid species in a 2:1:1:3:2:1 molar ratio), DOTAP−DOPC−DLPC−DC-Chol−DOPE−DMPC (black down-triangle, lipid species in a 2:1:1:4:3:1 molar ratio), DOTAP−DC-Chol−DOPE (white down-triangle, lipid species in a 1:1:2 molar ratio), DC-Chol−DMPC (gray down-triangle), DC-Chol−DOPE−DMPC (black diamond, lipid species in a 2:1:1 molar ratio), and DC-Chol−DOPE (white diamond). Where not specified, lipid species are in an equimolar ratio. The solid line is the fit to the data obtained by applying eq 3. Vertical dashed lines identify three different regimes of membrane charge density. In the first one, TE increases as a function of σ_M, but in the third one, it definitely decreases. The fwhm of the Gaussian curve-fitting TE data identify the regime of optimal membrane charge density. Each TE data point represents an average value of at least four experimental observations. Errors for TE are listed in Table 1.
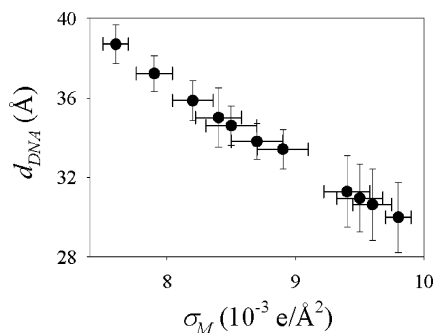

Figure 6. Experimental DNA−DNA distances plotted against membrane charge density, σ_M, as calculated by eq 2.

density was found to increase (i.e., d_{DNA} decreased) as a function of increasing σ_M (Figure 6).

Interestingly, Figure 5 shows that all TE data points merged onto a single experimental Gaussian curve

$$\text{TE} = \text{TE}_0 \exp-\left(\frac{\sigma_M - \sigma_M^*}{w}\right)^2 \qquad (3)$$

where $\text{TE}_0 = (1.9 \pm 0.2) \times 10^7$ RLU/mg protein, $\sigma_M^* = (8.8 \pm 0.2) \times 10^{-3}$ e/Å², and $w = (5.8 \pm 0.5) \times 10^{-4}$ e/Å.²

At first sight, our TE results resembled those of Ahmad et al.,[17] who showed that the TE profile versus σ_M of lamellar complexes is well described by a universal bell-shaped curve leading to the identification of an optimal transfection value, named σ_M^*, and three TE regimes. In the first region (regime A, Figure 5), corresponding to low σ_M, we observed an exponential increase in efficiency, but in the third regime, at high σ_M, efficiency decreased with increasing σ_M (regime C, Figure 5). The extension of the middle "optimal region" for $\sigma_M \approx \sigma_M^*$ (regime B, Figure 5) was estimated, according to ref 17, from the fwhm of the Gaussian curve-fitting TE data. Deeper insight into the TE data allowed us to identify striking differences between our results and those reported by Ahmad et al.[17] First, the optimal membrane charge density that we found ($\sigma_M^* \approx 9 \times 10^{-3}$ e/Å²) was much lower than that reported[17] ($\sigma_M^* \approx 17 \times 10^{-3}$ e/Å²). Second and most importantly, the extension of the optimal transfection regime ($w \approx 5 \times 10^{-4}$ e/Å²) is about 1 order of magnitude lower than that reported by Ahmad et al.[17] ($w \approx 6 \times 10^{-3}$ e/Å²). Even though a possible correlation with cell-type specificity cannot be excluded (Ahmad et al.[17] used mouse L-cells), other general aspects have to be considered. Gene delivery by lipoplexes is potentially regulated by a large number of physical parameters such as the lipoplex structure, membrane charge density, and cationic lipid/DNA charge ratio, ρ. Nevertheless, because the structure and charge ratio were the same as those reported by Ahmad et al.,[17] such physical parameters could not be taken into account to explain the observed discrepancy in the TE profile. It has recently been shown that the structure of lipoplexes can be altered by interaction with cellular anionic lipids and that the phase behavior of lipoplexes controls their TE values.[18,19,22] Anionic lipids can destroy the lipid bilayer converting the liquid-crystalline lamellar phase L_α into an inverted hexagonal or cubic phase. In an effort to interpret our TE data, we investigated the interaction of lipoplexes with anionic lipids. We were particularly interested in whether the structural changes in lipoplexes might correlate with the TE data reported above. To this end, we mixed lipoplexes and anionic liposomes (models of cellular membranes) made of DOPG, an anionic lipid commonly found in mammalian cells, in particular, in lysosomal membranes and mitochondrial inner membranes. The SAXD pattern of pure DOPG (Figure 7) displayed five diffraction peaks indexed as the (00l) reflections of a lamellar phase with 131.2 Å structural unity. The WAXD pattern ($1.2 < q < 1.6$ Å⁻¹) corresponding to the in-plane packing
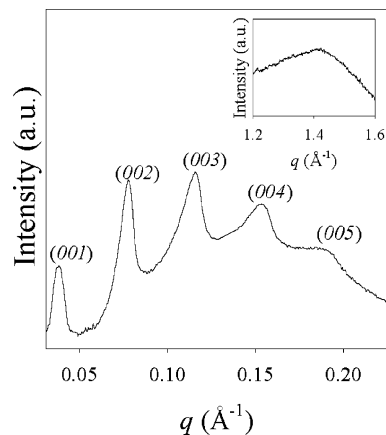

Figure 7. SAXD pattern of DOPG. Lamellar Bragg reflections (00l) are indicated. The corresponding wide-angle diffraction pattern showing the in-plane order of the hydrocarbon chains is given in the inset.
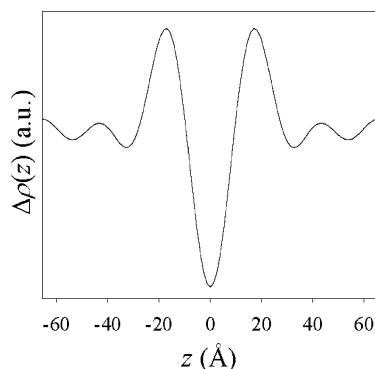
Figure 8. Electron density profile along the normal to DOPG bilayers from which the membrane thickness ($d_B = 34.1$ Å) and the water layer thickness ($d_W = 97.1$ Å) can be derived.

of the hydrocarbon chains (Figure 7, inset) confirmed that the system was in the fluid L_α phase. The calculated electron density profile over the unit cell of the DOPG bilayer is shown in Figure 8, where the more electron dense regions (i.e., the two central maxima) correspond to the DOPG headgroups. From the electron density profile of Figure 8, both the thickness of the DOPG bilayer ($d_B = 34.1$ Å) and that of the interbilayer water region ($d_W = 97.1$ Å) were calculated. These values are in good agreement with those previously reported for negatively charged POPG liposomes in the bulk by Pozo-Navas and co-workers.[46] The large lamellar periodicity, d, shows that the bilayers were in a highly swollen state where the unscreened double-layer repulsion seems to result in a highly repulsive interbilayer separation. Thus, the anionic lipid had the capacity to imbibe water and to swell while maintaining its lamellar structure. However, the SAXD pattern of DOPG is dominated by strong quasi-Bragg peaks demonstrating that the bilayers were in a highly bound state. The unexpected long scattering correlation length, indicated by the high number of diffraction maxima visible on the SAXD patterns, may be easily rationalized by considering that the centrifugation of capillaries consolidated the sample and facilitated the collapse of isolated membranes onto one another.

After the addition of negatively charged DOPG liposomes to the preformed lipoplexes, the structural organization of the membranes changed remarkably. Most importantly, we found evidence for the existence of three different stages. In the first stage ($0 < R < 1$), SAXD patterns of lipoplexes changed, but the lamellar structure of lipoplexes was essentially preserved. Figure 9 shows the structural evolution of A/DNA lipoplexes upon interaction with anionic lipids in the narrow range of anionic/cationic charge ($0 < R < 0.2$). SAXD measurements indicated that the DNA lattice was diluted by anionic lipids. This can be seen in SAXD scans where d_{DNA} changes from 42.6 Å at $R = 0$ up to 51.4 Å at $R = 0.2$. Here we emphasize that this was the first time that the shift of the DNA peak, caused by interaction with anionic lipids, was observed by SAXD experiments. In a recent paper,[22] we showed that 1D DNA packing density may be used to estimate the molar fraction of DNA released from lipoplexes by anionic lipids, X_{DNA}. When anionic lipids diffuse into the complex, they may form ionic charge pairs with cationic lipids, thus modifying the actual composition of cationic membranes. Because each ionic charge pair can be regarded as being made of two neutrally charged lipids, the actual percentage of neutral lipid in the bilayer, Φ', monotonously increases with increasing R. At the same time, the neutralization of cationic charge carried by cationic lipids and DNA released from
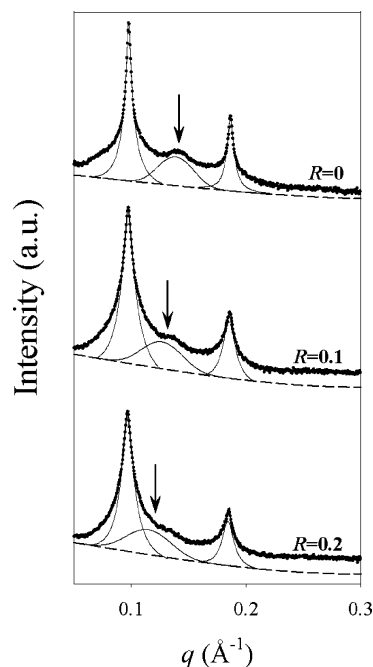

Figure 9. SAXD pattern of DOTAP−DOPC/DNA (A/DNA) lipoplexes as a function of increasing anionic/cationic charge ratio, R. Whereas the lamellar d spacing remains the same, the DNA−DNA distance, d_{DNA}, increases. This indicates that the 1D DNA in-plane rod lattice is progressively diluted by DOPG. The dashed lines are the backgrounds, and the solid lines show the best fitting functions to diffraction peaks.

Table 3. Comparison between the Molar Fraction of Released DNA as a Function of Increasing R Calculated with Equation 4 (X_{DNA}^{th}) and Quantified by Means of Agarose Gel Electrophoresis Experiments (X_{DNA}^{exp})

R	X_{DNA}^{th}	X_{DNA}^{exp}
0	0	0
0.1	0	0
0.2	0	0
0.5	n.d.	0
1	n.d.	0.15
2	n.d.	0.60
5	n.d.	0.95

lipoplexes results in a continuous deviation of ρ from its nominal value. Here we underline that both the diffusion of anionic lipids into the complex and DNA release result in a lowering of the DNA packing density. We therefore used changes in the DNA packing density to estimate the molar fraction of released DNA, X_{DNA}, as a function of increasing R:[47]

$$X_{DNA}(R) = 1 - \frac{d_{DNA}(R=0)}{d_{DNA}(R)} \frac{(1-\Phi)}{(1-\Phi')}(1-R) \qquad (4)$$

Changes in DNA packing density (i.e., in DNA−DNA distances) as a function of R were therefore used to estimate the fraction of released DNA, X_{DNA} (Table 3). Analogous results (not reported) were obtained for all of the lipid/DNA complexes. Note that in the range investigated ($0 < R < 0.2$) the lamellar repeat distance, d, did not change significantly as a function of R so that a large part of the DNA remained tightly bound to lipid bilayers. In cationic lipid/DNA complexes, DNA molecules fill the space between cationic membranes, suppress lipid bilayer fluctuations, and reduce the irregular variations typical of

(46) Pozo-Navas, B.; Raghunathan, V. A.; Katsaras, J.; Rappolt, M.; Lohner, K.; Pabst, G. *Phys. Rev. Lett.* **2003**, *91*, 028101.

(47) Caracciolo, G.; Pozzi, D.; Amenitsch, H.; Caminiti, R. To be submitted for publication.

multibilayer stacks. As a result, the long-range order along the normal to the lipid bilayer increases, and the "second-order disorder" in the crystal lattice decreases.[9,48] A direct comparison of the diffraction patterns of Figure 9 shows that a decrease in height is also accompanied by a progressive broadening of diffraction peaks as a function of increasing R. The width of a diffraction peak is related, among other things, to the size of the domains from which the diffraction comes.[49] We have therefore used the fwhm of the (001) Bragg reflection to estimate the average domain size of the multilayers and the DNA arrays, L_m, using the following relation[9]

$$L_m = \frac{2\pi}{\Delta q} \qquad (5)$$

where Δq is the fwhm of the (001) diffraction peak in q space. For the calculation, we used $\Delta q = \sqrt{(\text{fwhm})^2_{exp} - (\text{fwhm})^2_{beam}}$ where $(\text{fwhm})_{exp}$ is the experimental width of the (001) diffraction peak and $(\text{fwhm})_{beam}$ is the width of the intrinsic instrumental resolution function $((\text{fwhm})_{beam} \approx 6 \times 10^{-4}$ Å$^{-1})$. Using eq 5, we have determined that L_m is about 5000 Å with no anionic lipid added ($R = 0$) and this value is comparable to those of other cationic lipid/DNA complexes.[9] A significant dependence of the average multilayer domain size was found because it decreased to 2300 and 1900 Å for $R = 0.1$ and 0.2, respectively. This finding confirmed that adding anionic lipids gradually destabilizes the multilamellar structure of lipoplexes.

In the second stage, starting from $R \approx 1$, a major reorganization of the initial multilamellar structure of lipoplexes subsequent to their interaction with anionic lipids was observed. Here, experiments with A/DNA and BD/DNA lipoplexes are presented because these lipid formulations provided the clearest evidence of structural differences upon interaction with anionic lipids. Figure 10 shows SAXD patterns of A/DNA lipoplexes as a function of R. On the SAXD pattern of A/DNA with DOPG, diffraction maxima of the L_α^C phase were visible up to $R = 1$. This indicates that for $0 < R < 1$ the fluid bilayer of A membranes accommodated DOPG molecules within the lipid bilayer. A characteristic feature of this system was the extensive swelling of the lamellar phase that accompanied its enrichment with anionic DOPG (from $d \approx 65$ Å at $R = 0$ up to $d \approx 70.6$ Å at $R = 1$). For $R > 1$, the system underwent a phase transition where disintegration of the initial structure of A/DNA lipoplexes appeared. This was ascribed to the progressive disintegration of A membranes by DOPG molecules. We defined R^* as the anionic/cationic charge ratio at which lipid bilayer disintegration was complete. In the regime of phase coexistence ($1 < R < R^* = 4$), the SAXD pattern of the A/DNA/DOPG mixture (not reported) was increasingly dominated by the lamellar phase of pure DOPG. Further increase in the anionic lipid ($R > 4$) leads to the third one-phase stage where the system was identified as being in the L_α phase of pure DOPG. Structural changes induced by anionic lipids strictly depended on the lipid composition of lipoplexes. Taking into account the large differences in the chemical structures of lipids used (packing parameters, chain lengths, chain melting temperature), it was not surprising to observe that each lipid formulation exhibited a specific affinity for anionic lipids. For instance, a four-carbon difference in the carbon number is usually enough to induce the phase separation of lipids.[50] Recently, it has also been shown that cationic lipid derivatives having the
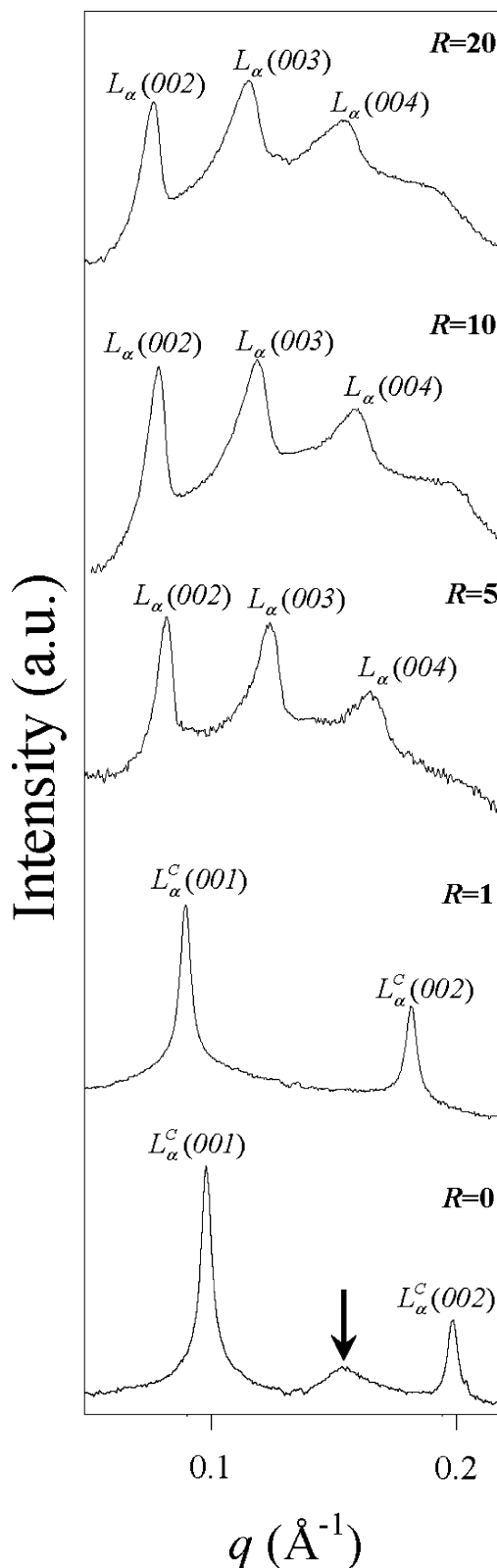
(48) Blaurock, A. E. *Biochim. Biophys. Acta* **1982**, *650*, *167*.
(49) Zhang, R. T.; Suter, R. M.; Nagle, J. F. *Phys. Rev. E* **1994**, *50*, 5047.
(50) Ollivon, M.; Lesieur, S.; Grabielle-Madelmont, C.; Paternostre, M. *Biochim. Biophys. Acta* **2000**, *1508*, 34.

Figure 10. SAXD pattern of DOTAP−DOPC/DNA (A/DNA) lipoplexes as a function of increasing anionic/cationic charge ratio, R, from the bottom to the top. At $R = 0$, lipoplexes are assembled into the lamellar phase. At $R > 1$, the lamellar phase starts being destroyed by anionic lipids At $R = 5$, only the lamellar phase of pure DOPG appears in the pattern.

same headgroup but different hydrophobic chains exhibit different transfection efficiencies.[51] Binary lipid mixtures of cationic derivatives transfected cells more efficiently than did separate lipids. Such a phenomenon has been assumed to be related to

a higher probability for packing defects, resulting in facilitated DNA release and/or to better compatibility with the cell membrane.

The phase behavior of BD/DNA lipoplexes is displayed in Figure 11. As evidence, the lamellar phase of BD/DNA lipoplexes was found to be much more resistant than that of A/DNA complexes. Indeed, whereas at $R = 5$ the lamellar phase of A/DNA complexes was completely destroyed, that of BD/DNA lipoplexes was still strong and dominant. On the SAXD pattern of BD/DNA lipoplexes at $R = 5$, the (003) Bragg peak of DOPG was the only visible reflection of the emerging new phase. What is interesting is that at $R = 20$ the lamellar lipid/DNA complex resisted disintegration by DOPG and was still present within the sample. In principle, one may ascribe this to the presence of cholesterol within the lipid bilayer of BD membranes. Recent studies emphasized the important role of cholesterol-based molecules for the formation of resistant patches in the membranes.[52] In particular, the liquid-ordered states induced by cholesterol in DMPC and DPPC aqueous dispersions were found to resist disintegration by a variety of detergents and fatty acids.[53] In our case, this suggestion was not compelling. Indeed, we observed that B/DNA and D/DNA lipoplexes, although having the same percentage of DC-Chol within the lipid bilayer as that of BD/DNA lipoplexes, were definitely less resistant to disintegration than BD membranes (data not reported).

After the complete disintegration of the lamellar phase of lipoplexes by anionic lipids, only the lamellar phase of DOPG was observed. The final structures of all samples (not reported) were only slightly perturbed by the initial lipid composition of lipoplexes (minor changes in lamellar d spacing). This finding indicated that cationic and neutral lipids forming lipoplexes ended up within the final structure containing excess DOPG.

To provide direct evidence for DNA release from lipoplexes after interaction with anionic liposomes, electrophoresis experiments on agarose gels were carried out as a function of increasing R. As well-clarified by Wang et al.,[51] the gel electrophoresis assay allows us to determine how much DNA is completely free from lipid while a fluorescence resonance energy transfer assay may overestimate the DNA release because it includes DNA that is no longer electrostatically associated with cationic lipids but still entrapped within the lipid aggregate. Figure 12 shows the digital photograph of A/DNA lipoplexes. As evident, the amount of free DNA (intensity of DNA bands) increased with increasing R (from left to right). The molar fraction of DNA released was quantified by means of dedicated software, and the obtained values are reported in Table 3. As evidence, they were in close agreement with those calculated using eq 4 (for $0 < R < 0.2$). Electrophoresis seems to suggest that DNA release from lipoplexes by DOPG may be a two-step process: in the first step ($0 < R < 1$), anionic lipids penetrate the cationic membranes of lipoplexes and neutralize the positive charge carried by cationic lipids, but DNA is not released. As a result, the enlargement of the 1D DNA in-plane lattice was due to the penetration of anionic lipids increasing the total membrane area. In the second step ($R > 1$), when enough cationic charge has been neutralized and the cationic lipid/DNA interaction has become sufficiently weak, DNA can start to escape from lipoplexes. We also observed (data not reported) that at each R value the amount of free DNA varied significantly with lipid formulation: the more stable the
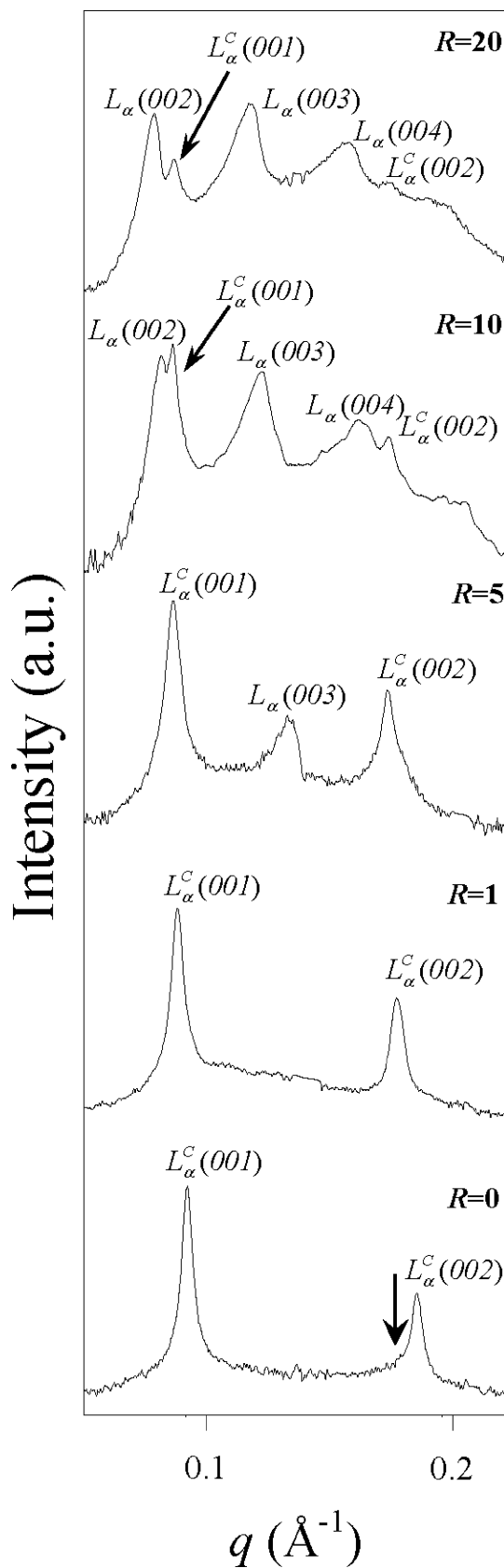
(51) Wang, L.; Koynova, R.; Parikh, H.; MacDonald, R. C. *Biophys. J.* **2006**, *91*, 3692.

(52) Mukherjee, S.; Ghosh, R. N.; Maxfield, F. R. *Physiol. Rev.* **1997**, *77*, 59.

(53) Chabaud, P.; Camplo, M.; Payet, D.; Serin, G.; Moreau, L.; Barthelemy, P.; Grinstaff, M. W. *Bioconjugate Chem.* **2006**, *17*, 466.

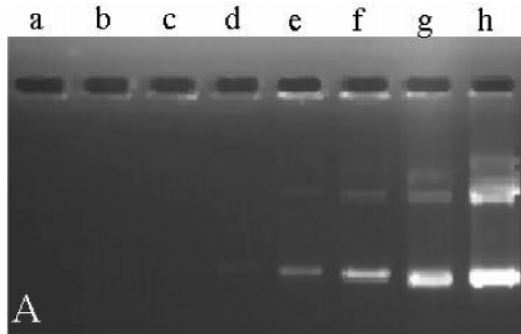(54) Pantazatos, D. P.; MacDonald R. C. *J. Membr. Biol.* **1999**, *170*, 27.

Figure 11. SAXD pattern of DC-Chol−DOPE−DMPC/DNA (BD/DNA) lipoplexes as a function of increasing anionic/cationic charge ratio, R. This lipid formulation was found to be the most resistant to disintegration by anionic lipids. Indeed, at $R = 20$, traces of the starting lamellar phase can be seen ($L_\alpha^C(00l)$).

structure of lipoplexes, the lower the extent of DNA released. In the case of A/DNA lipoplexes, the completion of DNA release

Figure 12. Digital photograph of DOTAP−DOPC/DNA lipoplexes (A/DNA). DOTAP−DOPC/DNA/DOPG systems were prepared with increasing anionic/cationic molar ratio: $R = 0$ (lane a), $R = 0.1$ (lane b), $R = 0.2$ (lane c), $R = 0.5$ (lane d), $R = 1$ (lane e), $R = 2$ (lane f), $R = 5$ (lane g), and control DNA (lane h). Experiments revealed two major bands for naked DNA (lane h). The high-mobility band was attributed to the most compact (super-coiled) form, and the less-intense one was considered to be the non-super-coil content in the plasmid preparation.
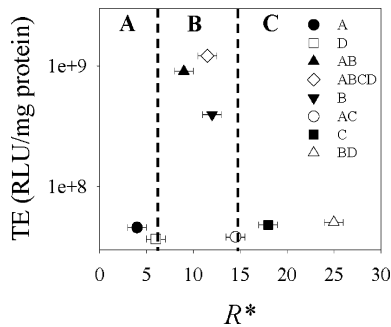

Figure 13. TE in RLU per milligrams of cellular protein plotted as a function of R^*, which is intended to be the anionic/cationic charge ratio at which the disintegration of the lamellar phase of the lipoplexes is complete. Each TE data point represents an average value of at least four experimental observations. Errors for TE are listed in Table 1.

occurred just at $R \approx 5$ (Table 3). This value is, within experimental error, in good agreement with R^* as determined by SAXD (Figure 5). This indicates that when the lamellar phase of lipoplexes was completely destroyed (as revealed by SAXD) then DNA was almost completely released. We therefore emphasize that electrophoresis experiments proved the existence of the assumed correlation between the destabilization of lipoplexes and DNA unbinding.

Given the complexity of the lipoplex−AL system, it is remarkable that the data coalesced into a convex curve when plotted against R^* (Figure 13). The new TE curve of Figure 13 exhibits three well-defined regimes of stability. Regime A, corresponding to unstable complexes, features an exponential increase in efficiency of over 2 orders of magnitude with increasing R^*. Regime C, corresponding to highly stable complexes, is characterized by a decrease in efficiency with growing R^*. Figure 13 also shows the existence of an intermediate regime (regime B) corresponding to the highest TE. This regime appeared to be like the region of optimal stability. Endocytosis is the dominant mechanism of entry of lamellar lipoplexes, as evident in recent work.[52,53] After cellular uptake via endocytosis, lipoplexes must escape from endosomes in order for DNA to move toward the cell nucleus. As Figure 13 clearly shows, inefficient lipoplexes were unstable against disintegration by anionic lipids (regime A, Figure 13) and released DNA upon adhering to anionic vesicles. This may suggest that unstable lipoplexes fuse with the endosomal membrane and dissociate
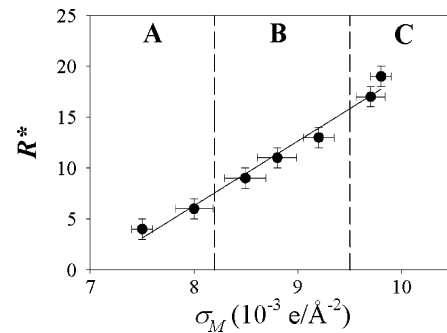

Figure 14. Profile of R^* as a function of membrane charge density, σ_M. Interestingly, R^* varies almost linearly with σ_M: the higher the membrane charge density of lipoplexes, the more resistant their structure.

early in the cytoplasm, where naked DNA can be easily digested by enzymes in which the cytoplasm is rich. Rapid escape from the endosome might be unfavorable because it would prevent the complex from taking advantage of the trafficking of endosomes toward the nucleus. At high R^*, lipoplexes were found to be inefficient, suggesting that high stability may also be an obstacle to successful DNA delivery by lamellar CL-DNA complexes. The maximum TE in the regime of optimal stability (regime B, Figure 13) is a sign of the compromise between opposing requirements: the structural instability of complexes may be disadvantageous because of the quick dissociation of complexes in the cytoplasm whereas high stability may be at the origin of the endosomal entrapment of lipoplexes. Bearing in mind that for efficient delivery DNA must be retained until the lipoplex is in the vicinity of the nucleus, the stability of lipoplex structures is likely responsible for the successful transfer of DNA into the cell nucleus. When the membrane charge density is plotted against R^*, a linear trend appears (Figure 14). This indicates that structural stability is strictly connected to membrane charge density.

Because interaction between oppositely charged membranes is likely to involve some local contact, charge densities of lipoplexes and anionic liposomes are expected to play a key role in membrane interaction, contact, and fusion. Whatever the fusion mechanism is, our finding that the interaction between lipoplexes and DOPG liposomes strictly depends on the membrane charge density of lipoplexes is consistent with many previous observations. The adhesion−condensation mechanism, first proposed by Kozlov and Markin,[55] predicts that interactions between oppositely charged macromolecules critically depend on the surface charge density. Other experimental observations made it clear that the magnitude of the net membrane charge density is the most important property in determining vesicle interactions.[56] Recently, Hed and Safran predicted the conditions under which two oppositely charged membranes show attractive instability.[57] These dynamic instabilities may be the precursors of membrane fusion (indispensable prerequisite for endosomal escape) in systems where artificial vesicles are engulfed by biological cells of opposite charge. Two layers with unequal charges of opposite sign can repel or be stable when in close proximity to each other. Attractive instability, described by Hed and Safran,[57] resulting in membrane fusion was found to be largely dominated by charge density patterns of approaching vesicles.

What we have shown here, which was poorly appreciated, is that the structural stability of lipoplexes is definitely well

(55) Kozlov, M. M.; Markin, V. S. *Gen. Physiol. Biophys.* **1984**, *5*, 379.
(56) Pantazatos, D. P.; Pantazatos, S. P.; MacDonald, R. C. *J. Membr. Biol.* **2003**, *194*, 129.
(57) Hed, G.; Safran, S. A. *Phys. Rev. Lett.* **2004**, *93*, 1.

correlated with their membrane charge density. On the basis of the most accredited evidence reported in the literature so far, our findings seem to suggest that the membrane charge density, at least in the investigated range ($0.007 < \sigma_M < 0.01$ e/Å^2), regulates the interaction between cationic lipoplexes and anionic vesicles and most likely controls membrane fusion. Indeed, all membrane charge densities investigated in the present article lie in Regime I of Ahmad et al.,[17] where the ability of lipoplexes to fuse with the anionic endosomal membrane is the factor limiting TE. In this context, varied structural stability is the "observable consequence" of the varied extent of membrane fusion regulated by the membrane charge density. At low σ_M, anionic liposomes are able to interact with lipoplexes effectively, completely neutralize the positive charge of cationic lipids, destroy the L_α^C phase, and promote DNA escape from endosomes. At high σ_M, we therefore hypothesize that TE is strongly limited by a reduced fusion of lipoplexes with endosomes in the cytoplasm as a result of the electrostatic interactions between the lipid bilayers and the DNA becoming more intense with increasing σ_M.[17] Differences in TE observed for the various mixtures here reported would therefore be caused by differences in the ability of lipoplexes to fuse with the endosomal membrane.

The schematic reported in Figure 15 summarizes a possible mechanism occurring in the early stages of internalization of the lipoplex within the cell. Electrostatic attractions let the lipoplex approach the anionic surface of the cell, and attachment is followed by endocytosis, resulting in endosomal entrapment.[10] Our experiments suggest that the less stable lipoplexes dissociate early in the cytoplasm where naked DNA may be easily digested by enzymes in which the cytoplasm is rich. As a result, unstable lipoplexes are slightly efficient (Figure 5) because the lipoplex might dissociate in the cytoplasm instead of in the nuclei.[53] Optimally, stable lipoplexes may release delivered DNA slowly in the cytoplasm, with the event occurring through interactions with anionic proteins that readily form complexes with cationic vesicles. Overly stable lipoplexes remain trapped within endosomes and do not allow for complete DNA release, therefore resulting in a decrease in TE. The study presented here focuses on one particular cell line, but TE experiments showed similar trends in A-17 cancer cell lines.[58,59]

Conclusions

We have investigated the structure−efficiency relationship of lamellar lipoplexes. Of primary significance is the discovery that high TE can be achieved with multicomponent complexes at low membrane charge density ($\sigma_M < 9 \times 10^{-3}$ e/Å^{-2}); this had never before been achieved with binary lipoplexes. By investigating the interaction between lipoplexes and anionic membranes (models of cellular membranes), we could identify the basis of the different powerful ability of lipoplexes: we have

(58) Galiè, M.; D'Onofrio, M.; Montani, M.; Amici, A.; Calderan, L.; Marzola, P.; Benati, D.; Merigo, F.; Marchini, C.; Sbarbati, A. *Neoplasia* **2005**, *7*, 528.
(59) Galiè, M.; Sorrentino, C.; Montani, M.; Micossi, L.; Di Carlo, E.; D'Antuono, T.; Calderan, L.; Marzola, P.; Benati, D.; Merigo, F.; Orlando, F.; Smorlesi, A.; Marchini, C.; Amici, A.; Sbarbati, A. *Carcinogenesis* **2005**, *26*, 1868.
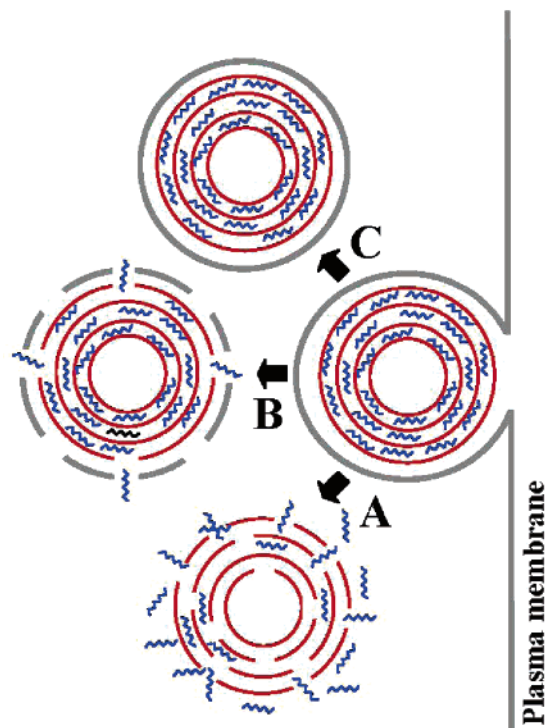

Figure 15. Proposed mechanism of the interaction of lipoplexes (labeled as CL/DNA) with the anionic plasma membrane of the cell. Electrostatic attractions let the lipoplex approach the anionic surface of the cell, and attachment is followed by endocytosis, resulting in endosomal entrapment. The solid gray line represents a portion of the plasma membrane separating the inner and outer space of a cell. The less stable the lipoplexes, the earlier the dissociation of DNA in the cytoplasm (A). When naked, DNA may be easily digested by enzymes in which the cytoplasm is rich. Optimally stable lipoplexes (B) may release delivered DNA slowly into the cytoplasm, the event occurring through interactions with anionic proteins that readily form complexes with cationic vesicles. Lipoplexes that are too stable (C) do not fuse with the endosomes and do not allow for DNA release. Endosomal entrapment therefore results in a decrease in transfection efficiency.

established structural stability upon interaction with anionic molecules (cellular lipids and proteins) as a key parameter governing the transfection efficiency of lipoplexes. Our results provide a physical basis for the rational design of novel cationic lipid formulations. Future work will be carried out to confirm this hypothesis and to determine whether other effects, such as the specificity of lipid formulations and cell lines, may play a role in lipid-mediated gene delivery. The future adoption of rationally designed lipoplexes offering protection against disintegration by anionic lipids would ensure that users definitely improve the transfection efficiency of lipid carriers.